Inorganic Chemistry

pubs.acs.org/IC

Article

Vapor-Phase Loading of an Ionic Liquid into a Zeolitic Imidazolate Framework

Martin Obst, Max L. Tietze, Aleksander Matavž, Sabina Rodriguez-Hermida, Kristof Marcoen, Tom Hauffman, and Rob Ameloot*

Cite This: *Inorg. Chem.* 2022, 61, 17137−17143

Read Online

ACCESS | Metrics & More | Article Recommendations | Supporting Information

ABSTRACT: Composites formed by a metal−organic framework (MOF) and an ionic liquid (IL) are potentially interesting materials for applications ranging from gas separation to electrochemical devices. Consequently, there is a need for robust and low-cost preparation procedures that are compatible with the desired applications. We herein report a solvent-free, one-step, and vapor-based ship-in-bottle synthesis of the IL@MOF composite 1-butyl-3-methylimidazolium bromide@ZIF-8 in powder and thin film forms. In this approach, volatile IL precursors evaporate and subsequently adsorb and react within the MOF cages to form the IL.

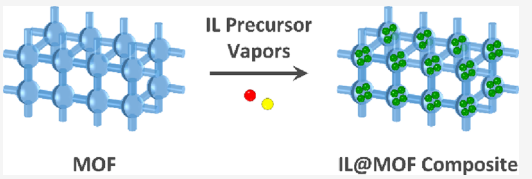

INTRODUCTION

Incorporating an ionic liquid (IL) into the pores of a metal−organic framework (MOF) leads to composites (IL@MOF) with potential applications in gas separation and storage, catalysis, and electrochemical devices.[1−4] Since IL@MOF composites combine the properties of MOFs and ILs, their adsorption properties and ionic conductivity can be considerably different from those of the parent MOF material.[1] For instance, the composite [bmim]PF_6@ZIF-8 shows double the CO_2/N_2 adsorption selectivity compared to ZIF-8.[5] Ionic conductivity even below the IL freezing temperature was achieved by incorporating [emim]NTf_2 into ZIF-8.[6] Incorporation of an IL can also render the MOF meltable, as demonstrated for [emim]NTf_2@ZIF-8.[7] Moreover, IL@MOF catalysts can be easily separated from the reaction mixture, which is not possible for pure ILs.[1,8]

Three major approaches are followed for the preparation of IL@MOF composites: (i) IL diffusion into the MOF pores (i.e., wet impregnation in a solvent or solvent-free mixing using mortar and pestle);[9−16] (ii) the ionothermal synthesis of the MOF, where the IL acts as both a solvent and a structure-directing agent and either the anion or the cation is incorporated in the pores;[17−21] and (iii) the ship-in-bottle (SIB) method,[22−25] in which the IL is formed inside the MOF pores. Among these methods, the SIB method is particularly favorable because it can overcome the problem of IL leaching from the MOF for a well-chosen guest−host pair. In this approach, small IL precursors are sequentially diffused into the pores, where they react to form the IL. The IL becomes sterically trapped when it is larger than the pore aperture.[1] Thus far, the SIB method has been only performed in solution or in a neat liquid precursor.

A drawback common to all preparation methods reported thus far is that they are liquid-phase processes that require a solvent or a relatively large volume of the precursor or IL. Furthermore, high IL loadings may be difficult to achieve due to competition with solvent molecules.[26] On the other hand, the loading of guest molecules into a MOF can be simply performed from the vapor phase. Examples are the confinement of anthracene in ZIF-8 by sublimation[26] and the loading of organometallic compounds such as ferrocene into MOF-5.[27] However, the direct loading of ILs into a MOF from the vapor phase is impractical because of their low vapor pressure ($<10^{-3}$ mbar at moderate temperatures), and the requirement of an ultrahigh vacuum ($<10^{-8}$ mbar).[28,29] Nevertheless, several common ILs can be easily synthesized from volatile precursors. For example, imidazolium ILs are formed by the quaternization of an imidazole with an alkyl halide even under solvent-free conditions and at moderate temperatures.[30,31] Recently, we exploited this reaction to develop the chemical vapor deposition of ILs on surfaces, resulting in ionogel thin films and patterns.[32] In that study, two volatile precursors were sequentially evaporated and diffused into a polymer film, where they reacted to form the IL. The polymer acted as a reservoir for the precursors and allowed area-selective ionogel formation. In this work, we expanded this approach to load the IL 1-butyl-3-methylimidazolium bromide ([bmim]Br) into powder and thin film forms of ZIF-8 via a novel vapor-phase ship-in-bottle (VSIB) method (Figure 1a).

Received: July 22, 2022
Published: October 19, 2022

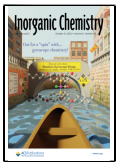

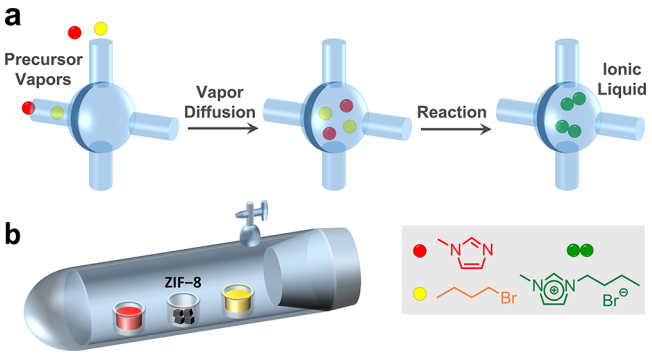

Figure 1. Vapor-phase ship-in-bottle (VSIB) method. (a) Schematic representation of the VSIB method in a MOF pore. Note the simultaneous introduction of both precursors. (b) Illustration of the Schlenk flask setup used for the VSIB method. The inset shows the structures of the precursors 1-methylimidazole and 1-bromobutane and the resulting IL [bmim]Br.

RESULTS AND DISCUSSION

ZIF-8 consists of Zn^{2+} ions connected by 2-methylimidazolate linkers. The framework has a sodalite topology consisting of 11.6 Å cages connected by small 3.4 Å aperatures.[26] Because of this topology, large molecules formed through the SIB method can be trapped inside the cages, resulting in a stable IL@MOF composite. For example, [bmim]Br was loaded into ZIF-8 using the conventional liquid-phase SIB method by sequentially suspending the MOF powder in the neat precursors 1-methylimidazole and 1-bromobutane.[23] In this study, [bmim]Br was selected as the target IL because both precursors were liquids with considerable vapor pressures and readily reacted via the quaternization of the non-methylated imidazole nitrogen atom.

ZIF-8 crystals with particle sizes below 1 μm were synthesized via a solvent-free method by heating a physical mixture of zinc oxide and 2-methylimidazole.[33] The ZIF-8 powder was then placed in a Schlenk flask together with the IL precursors in separate glass boats (Figures 1b and S1). The Schlenk flask was heated to 70 °C for 20 h to allow precursor evaporation, simultaneous diffusion into the MOF powder, and a subsequent reaction to form the IL.

Using this approach, [bmim]Br was successfully formed in the ZIF-8 cages, as confirmed by solution ^{1}H NMR spectrum of the acid-digested product (Figure 2a; for peak assignments, see Figure S2). Unreacted precursor molecules and [bmim]Br attached to the ZIF-8 surface were removed by washing the product in ethanol at room temperature. This washing step did not remove the [bmim]Br trapped inside the cages. ^{1}H NMR reveals an average loading of 2.7 [bmim]Br ion pairs per ZIF-8 cage (ip/c). To confirm the complete removal of surface-adsorbed [bmim]Br, samples of the MOF material were taken after each washing step and analyzed by ^{1}H NMR, which showed the [bmim]Br content was constant from the second washing step onward (Figure S3). Thermogravimetric analysis (TGA) revealed a mass loss of 28 wt % when the composite was heated to 300 °C. Under these conditions, the ZIF-8 host remains intact (Figure 2b) while the [bmim]Br guest dequaternizes to form volatile alkylimidazoles and alkyl bromides.[34] The observed mass loss is in good agreement with the loading calculated from NMR data (2.7 ip/c corresponds to 30 wt %). Powder X-ray diffraction of the product show the retention of the crystallinity of the ZIF-8 host upon loading (Figure 2c). Furthermore, the increase in the intensities of the (200) and (211) diffraction peaks relative to that of the (110) reflection is indicative of [bmim]Br loading; a similar effect was previously observed for the loading

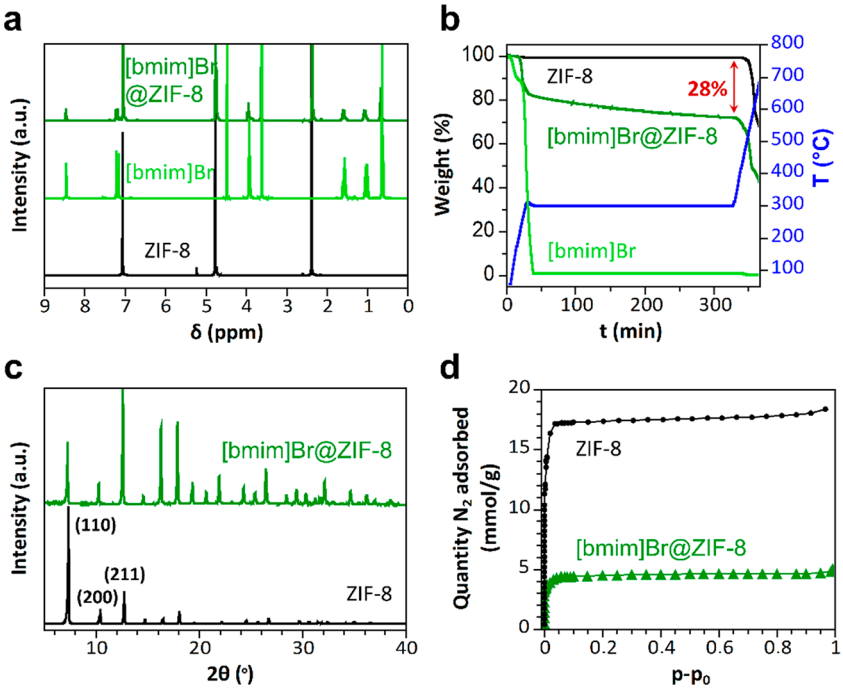

Figure 2. Characterization of [bmim]Br@ZIF-8 obtained by the VSIB method. (a) ^{1}H NMR spectra of ZIF-8 and [bmim]Br@ZIF-8 in DCl/D_2O. (b) TGA curves of ZIF-8, [bmim]Br@ZIF-8, and [bmim]Br (bulk, for comparison). (c) PXRD patterns of ZIF-8 and [bmim]Br@ZIF-8. (d) N_2 physisorption isotherms of ZIF-8 and [bmim]Br@ZIF-8 at 77 K. The BET specific surface areas of ZIF-8 and [bmim]Br@ZIF-8 are 1671 and 411 m^2/g, respectively.

https://doi.org/10.1021/acs.inorgchem.2c02615
Inorg. Chem. 2022, 61, 17137−17143

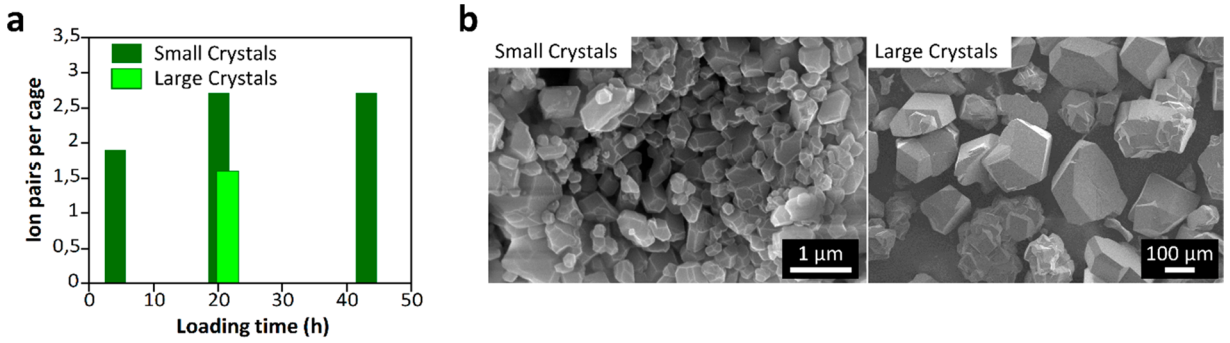

Figure 3. Influence of the ZIF-8 crystal size on the IL loading. (a) Number of IL ion pairs obtained per cage of ZIF-8. (b) SEM images of small and large ZIF-8 crystals used in VSIB experiments.

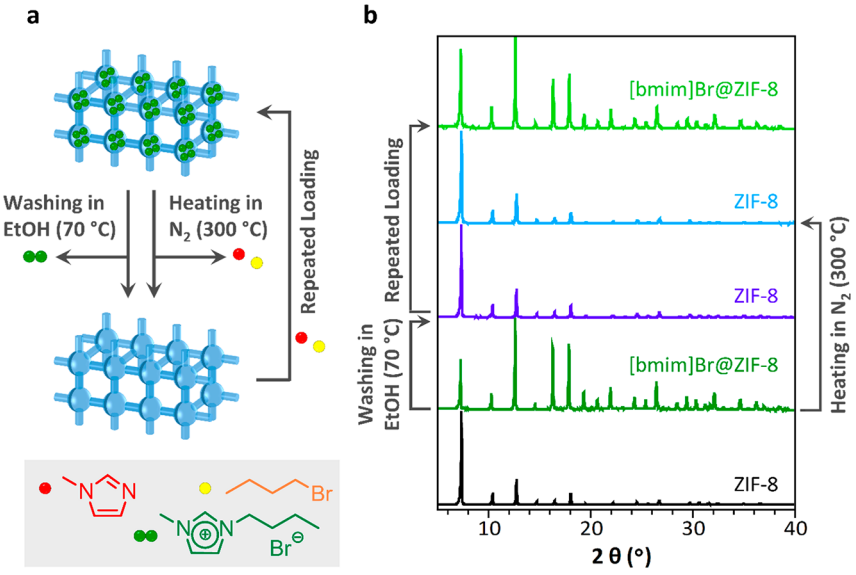

Figure 4. Reversibility of the VSIB IL loading. (a) [bmim]Br can be removed from ZIF-8 by washing the composite in EtOH at 70 °C or heating it in nitrogen at 300 °C. After the removal of the IL, ZIF-8 can be loaded again using the VSIB method equally well as the pristine material. (b) XRD patterns of ZIF-8 (size <1 μm), [bmim]Br@ZIF-8 (2.7 ip/c) after being washed in ethanol at 70 °C or heated at 300 °C in a N_2 stream, and [bmim]Br@ZIF-8 (repeated loading after [bmim]Br was washed out in ethanol, 2.8 ip/c).

of anthracene into ZIF-8.[26] Physisorption at 77 K reveals a lower amount of adsorbed nitrogen for the composite compared to empty ZIF-8, corresponding to a reduction of the BET specific surface area from 1671 to 411 m^2/g (Figure 2d).

A shorter reaction time (4 h vs 20 h) resulted in a lower IL loading (1.9 ip/c), whereas a longer reaction time (43 h) did not increase the loading beyond 2.7 ip/c (Figure 3a). Large ZIF-8 crystals (100−300 μm) obtained by solvothermal synthesis were also successfully loaded with [bmim]Br after 20 h of reaction. However, because of diffusion limitations, the overall loading could only reach 1.6 ip/c (Figure 3a). When the large crystals were ground into smaller particles, the obtained loading (2.7 ip/c) was the same as that for the smaller crystals. For the intact large crystals, the [bmim]Br loading did not change during the washing steps, indicating that all the IL was present within the MOF cages and no surface-adsorbed [bmim]Br was formed. Therefore, the washing step could be replaced by simply heating the sample to 120 °C in a vacuum to remove unreacted precursors, as confirmed by ^{1}H NMR spectroscopy.

[bmim]Br was removed without damaging the ZIF-8 host, as illustrated in Figure 4a. Although the [bmim]Br@ZIF-8 composite is stable in ethanol at room temperature, the IL guest can be removed by stirring the sample in hot ethanol (70 °C) for two days. Upon heating, the size of the ZIF-8 aperture increases, allowing the IL to diffuse out of the cage.[35,36] Throughout this treatment, ZIF-8 remains crystalline, and the relative intensities of the diffraction peaks are in agreement with the XRD pattern for pristine ZIF-8 (Figure 4b). Furthermore, as observed in the TGA analysis, [bmim]Br could also be removed via dequaternization to volatile alkylimidazoles and alkyl bromides by heating the sample to 300 °C in nitrogen (Figure 4b). Heating unloaded ZIF-8 as a control experiment resulted in neither any mass loss nor a loss of crystallinity.

The VSIB method can be extended to ZIF-8 films, which will facilitate the valorization of IL@MOF composites in microelectronics, ionic conductors, or microbatteries. Since both the MOF film and the IL can be deposited from the vapor phase, this approach meets the requirements of micro-technology fabrication (e.g., conformal, defect-free coatings with controlled thickness). Loading was performed in a Schlenk flask containing the ZIF-8 film and the IL precursors in separate glass boats at 70 °C (Figure S4). After being loaded with [bmim]Br, the film was heated to 110 °C to remove

https://doi.org/10.1021/acs.inorgchem.2c02615
Inorg. Chem. 2022, 61, 17137−17143

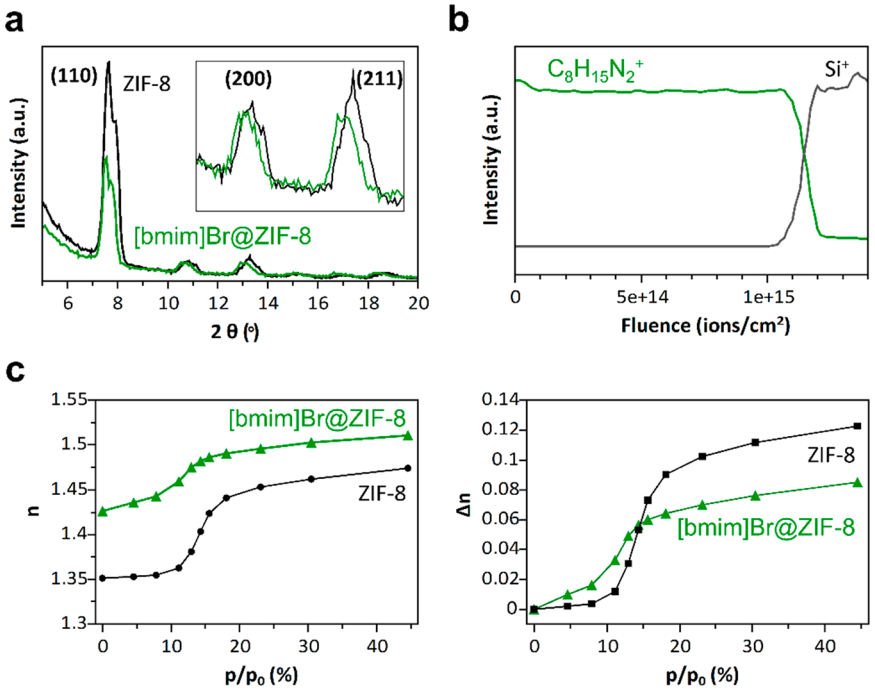

Figure 5. Characterization of [bmim]Br@ZIF-8 films obtained by the VSIB method. (a) GIXRD patterns of ZIF-8 and [bmim]Br@ZIF-8 films (inset shows magnified GIXRD $2\theta = 9.5—14.5$). (b) ToF-SIMS depth profile of the [bmim]Br@ZIF-8 film. (c) Methanol adsorption isotherms of ZIF-8 and [bmim]Br@ZIF-8 films; the refractive index was determined by ellipsometric porosimetry (left, n; right, Δn).

unreacted precursor molecules. Grazing-incidence X-ray diffraction demonstrates the crystallinity of the film (Figure 5a), and the change of the relative diffraction intensities indicates the presence of [bmim]Br. As indicated by time-of-flight secondary ion mass spectrometry (ToF-SIMS) depth profiling, [bmim]Br is homogeneously distributed over the ZIF-8 film; a constant signal of $C_8H_{15}N_2^+$ is detected upon sputtering until the film−substrate interface is reached (Figure 5b). Ellipsometry was used to determine the refractive index of the ZIF-8 film before and after IL loading. The [bmim]Br@ZIF-8 film has a refractive index of 1.426, which is considerably higher than that of the unloaded ZIF-8 film (1.351). The amount of [bmim]Br was calculated to be in the range of 2.8—3.4 ip/c (see the Experimental Section), which is similar to the value obtained for the powder samples. Ellipsometric porosimetry using methanol as a probe molecule[37] reveals that the porosity of the [bmim]Br@ZIF-8 film is lower than that of the unloaded ZIF-8 film, as would be expected (Figure 5c).

CONCLUSION

We have developed a novel vapor-phase approach for the preparation of [bmim]Br@ZIF-8 composites. Simultaneous diffusion of the precursor vapors into the cages of ZIF-8 leads to the formation of the target IL. In this way, efficient solvent-free, vapor-phase loading is enabled and problems related to the low vapor pressure of the target IL are bypassed. In contrast to the conventional SIB method in the liquid phase,[23,24] this vapor-phase approach requires only one step, avoids laborious washing, and is compatible with micro-fabrication methods.

EXPERIMENTAL SECTION

Materials. ZnO (particle size of 25 nm) was purchased from Roth; 2-methylimidazole was purchased from Sigma-Aldrich; zinc nitrate hexahydrate, 1-bromobutane, and sodium formate were purchased from Acros Organics; and 1-methylimidazole was purchased from Alfa Aesar and used without further purification.

Characterization. *^{1}H NMR.* ^{1}H NMR spectra were recorded on a Bruker Advance 300 MHz spectrometer. The ZIF-8 samples (ca. 5 mg) were dissolved in a solution containing DCl/D_2O (32 wt %, 50 μL) and 500 μL of D_2O or acetone-d_6. The loading amount (x) of [bmim]Br (ion pairs per cage) was calculated using eq 1

$$x = 12\frac{\text{Integral of [bmim]Br}}{\text{Integral of ZIF-8 linker}} \quad (1)$$

TGA. TGA was carried out on a STA 449 F3 Jupiter instrument in a nitrogen atmosphere (heated to 300 °C at 10 °C/min, isothermal heating at 300 °C for 5 h, and heated to 700 °C at 10 °C/min). The correlation between TGA mass loss and the loading amount (x) of [bmim]Br is given by eq 2 as follows:

$$\text{Mass Loss} = \frac{219x}{219x + 1378} \quad (2)$$

where the molar masses of [bmim]Br and one ZIF-8 cage are 219 and 1378 g/mol, respectively.

XRD. XRD measurements were performed on a Malvern PANalytical Empyrean diffractometer equipped with a PIXcel3D solid-state detector using a Cu anode.

SEM. SEM photographs were acquired on an FEI XL30FEG instrument after the samples were sputter-coated with 5 nm of Pt.

N_2 Sorption. N_2 sorption isotherms were recorded at 77 K using a Micromeritics 3Flex physisorption instrument. The samples were degassed before measurements at 120 °C under dynamic vacuum (10^{-2} mbar) for 3 h.

FTIR. FTIR measurements were performed on a Varian 670 Fourier Transform-IR spectrometer with a Ge crystal plate in the VeeMAX III module that was operated on attenuated total reflection geometry. A liquid-nitrogen-cooled mercury cadmium telluride detector was used.

ToF-SIMS. ToF-SIMS analysis was performed on a TOF.SIMS 5 instrument (ION-TOF GmbH). A 30 keV Bi_3^+ analysis beam (target current: 0.35 pA) was used in the high-current bunched mode for high mass resolution ($m\ \Delta m^{-1} \sim 8000$ at 29 u, $^{29}Si^+$). The primary

https://doi.org/10.1021/acs.inorgchem.2c02615
Inorg. Chem. 2022, 61, 17137−17143

ion dose was kept sufficiently low such that the static limit of 1×10^{13} ions cm^{-2} per analysis was not exceeded. During measurements, the pressure in the chamber was $\sim 3.4 \times 10^{-8}$ mbar. Depth profiles were obtained in a dual-beam configuration, where a 10 keV Ar_{1250}^{+} cluster ion beam (target current of 4.5 nA) was applied as a sputter beam. At the center of the 800 μm × 800 μm crater, a 100 μm × 100 μm area was analyzed.

Spectroscopic Ellipsometry. Spectroscopic ellipsometry was applied to determine the optical properties of unloaded and loaded ZIF-8 (J. A. Woollam, US). Ψ and Δ were recorded from 400 to 1000 nm at a 70° incident angle. Optical modeling was performed using the CompleteEASE 6.60 software (J. A. Woollam). A porous effective medium approximation (Porous EMA) model was used to estimate the pore-filling factor of IL within ZIF-8. First, the unloaded ZIF-8 film was measured and modeled using a Cauchy model ($n(\lambda) = A + B/\lambda^2$; $k = 0$) to determine the A and B coefficients of empty ZIF-8. The porosity, $\phi_{por} = 58.8\%$, was assumed according to ref 38, and the filling factor was kept at zero. For the IL-loaded sample, a Cauchy model was used to model the IL by applying the refractive index of the pure IL, $A = 1.54$.[39] The dispersion factor B was either fixed at zero or fitted, which gave about 10% variation in the fitted filling-factor value. The Cauchy coefficients of ZIF-8 were kept constant during the modeling of IL loading. The estimated filling factor was in the range from 27% to 37%, which was in a good agreement with the 34% methanol uptake reduction upon IL loading (Figure 5c). The loading (mmol/g) was calculated using eq 3 as follows:

$$\frac{n_{IL}}{m_{ZIF\text{-}8}} = \frac{V_{IL}}{V_{ZIF\text{-}8}} \frac{\rho_{IL}\phi_{por}}{M_{IL}\rho_{ZIF\text{-}8}} \quad (3)$$

where $\frac{V_{IL}}{V_{ZIF\text{-}8}}$ is the filling factor and M_{IL} is the molar mass of IL. The density of ZIF-8 ($\rho_{ZIF\text{-}8} = 0.95$ g cm^{-3}) was taken from ref 38. The density of the IL ($\rho_{IL} = 1.30$ g cm^{-3}) was taken from ref 39. The loading (ip/c) was calculated by assuming a unit cell volume of 4.924 nm^3.[40] Methanol adsorption isotherms of unloaded and IL-loaded films were measured using the iSE in combination with a stainless steel in situ gas cell and home-build vapor dosing equipment.[41]

Synthesis of ZIF-8. *Powder: Small Crystals.* ZnO (162 mg, 2.00 mmol) and 2-methylimidazole (481 mg, 5.85 mmol) were mixed and ground with a pestle and mortar. The mixture was heated at 110 °C in a synthesis oven for 1 d, washed with methanol three times, and subsequently dried.

Powder: Large Crystals. The procedure described in ref 42 was followed. $ZnNO_3{\cdot}6H_2O$ (3.528 g, 11.86 mmol) was dissolved in 40 mL of methanol. 2-Methylimidazole (1.944 g, 23.72 mmol) and sodium formate (0.807 g, 11.86 mmol) were dissolved in 40 mL of methanol. Both solutions were sonicated for 2 min, and the latter solution was poured into the former solution under stirring. The reaction mixture was stirred for 2 more minutes, then heated at 90 °C for 24 h in a sealed glass jar. The resulting crystals were removed from the wall by sonication, washed three times with methanol, and dried.

ZIF-8 Films. ZIF-8 thin films were synthesized using the deposition route described in ref 43. A 25 × 25 mm^2 silicon wafer was used as the substrate. Prior to ZIF-8 deposition, the substrate was cleaned in a piranha solution (H_2SO_4/H_2O_2 in 3:1 volume ratio) for 30 min at 70 °C and extensively washed with deionized water and methanol. Stock solutions of 25 mM zinc nitrate hexahydrate (Alfa Aesar, 99%) and 50 mM 2-methylimidazole (Acros Organics, 99%) were prepared separately in methanol. The deposition of the ZIF-8 layer was performed by combining 10 mL of each stock solution in a glass beaker and putting the substrate in the reaction mixture face-down. A plastic spacer ring about 5 mm thick was used to provide space between the bottom of the beaker and the substrate surface. After 30 min of reaction, the substrate was taken out of the reaction mixture and washed in methanol. The deposition step was repeated three times in total to yield a 310 nm thick ZIF-8 film. After the last layer deposition, the substrate was sequentially washed three times in methanol and once in ethanol, then dried under a nitrogen flow.

Vapor-Phase Loading of IL into ZIF-8. Powder. ZIF-8 (100 mg) was weighed into a glass boat, and 1-methylimidazole and 1-bromobutane (0.5 mL each) were filled into glass boats using a pipet. The three glass boats were transferred into a Schlenk tube (Figure S1). The tube was purged with nitrogen to achieve an inert atmosphere, placed in a synthesis oven, and heated at 70 °C for 20 h. Subsequently, ZIF-8 was washed by stirring it in ethanol four times (10 min—10 min—1h—1h, see Figure S3) and dried at 60 °C. The precursor/ZIF-8 ratio of 5 μL/mg could be reduced to 1 μL/mg, resulting in the same loading; a ratio of 0.5 μL/mg also resulted in a loading of 2.3 ip/c.

Film. The ZIF-8 film and the precursor vials (each containing 5 μL of the precursor) were glued on a glass slide. The glass slide was transferred into a Schlenk tube (Figure S4). The tube was purged with nitrogen to achieve an inert atmosphere, placed in a synthesis oven, and heated to 70 °C for 3 h. Subsequently, the ZIF-8 film was removed from the Schlenk vial and heated to 110 °C for 1 h to remove unreacted precursor molecules.

■ ASSOCIATED CONTENT

Supporting Information

The Supporting Information is available free of charge at https://pubs.acs.org/doi/10.1021/acs.inorgchem.2c02615.

Photographs of experimental setups, characterization of [bmim]Br@ZIF-8 powder samples (^{1}H NMR and FTIR), and additional experimental details (PDF)

■ AUTHOR INFORMATION

Corresponding Author

Rob Ameloot − *Center for Membrane Separations, Adsorption, Catalysis, and Spectroscopy (cMACS), KU Leuven, 3001 Leuven, Belgium;* orcid.org/0000-0003-3178-5480; Email: rob.ameloot@kuleuven.be

Authors

Martin Obst − *Center for Membrane Separations, Adsorption, Catalysis, and Spectroscopy (cMACS), KU Leuven, 3001 Leuven, Belgium;* orcid.org/0000-0002-9330-311X

Max L. Tietze − *Center for Membrane Separations, Adsorption, Catalysis, and Spectroscopy (cMACS), KU Leuven, 3001 Leuven, Belgium;* orcid.org/0000-0002-9018-3829

Aleksander Matavž − *Center for Membrane Separations, Adsorption, Catalysis, and Spectroscopy (cMACS), KU Leuven, 3001 Leuven, Belgium;* orcid.org/0000-0002-3385-3566

Sabina Rodriguez-Hermida − *Center for Membrane Separations, Adsorption, Catalysis, and Spectroscopy (cMACS), KU Leuven, 3001 Leuven, Belgium*

Kristof Marcoen − *Research Group of Electrochemical and Surface Engineering (SURF), Vrije Universiteit Brussel, 1050 Brussels, Belgium;* orcid.org/0000-0003-2831-483X

Tom Hauffman − *Research Group of Electrochemical and Surface Engineering (SURF), Vrije Universiteit Brussel, 1050 Brussels, Belgium*

Complete contact information is available at: https://pubs.acs.org/10.1021/acs.inorgchem.2c02615

Author Contributions

The manuscript was written through contributions of all authors. All authors have given approval to the final version of the manuscript.

Notes

The authors declare no competing financial interest.

https://doi.org/10.1021/acs.inorgchem.2c02615
Inorg. Chem. 2022, 61, 17137−17143

■ ACKNOWLEDGMENTS

We acknowledge funding from the European Union via the Horizon 2020 FETOPEN-1-2016-2017 research and innovation program (Grant 801464) and from the Research Foundation Flanders (FWO Vlaanderen) via research and infrastructure projects G0E6319N and I014018N. M.L.T. thanks the FWO for support from a senior postdoctoral fellowship (12ZK720N).

■ REFERENCES

(1) Kinik, F. P.; Uzun, A.; Keskin, S. Ionic Liquid/Metal-Organic Framework Composites: From Synthesis to Applications. *ChemSusChem* **2017**, *10* (14), 2842−2863.
(2) Yoshida, Y.; Kitagawa, H. Ionic Conduction in Metal-Organic Frameworks with Incorporated Ionic Liquids. *ACS Sustainable Chem. Eng.* **2019**, *7* (1), 70−81.
(3) Thomas, A.; Prakash, M. Ionic Liquid Incorporation in Zeolitic Imidazolate Framework-3 for Improved CO2 Separation: A Computational Approach. *Appl. Surf. Sci.* **2021**, *562*, 150173.
(4) Zhao, M.; Ban, Y.; Yang, W. Assembly of Ionic Liquid Molecule Layers on Metal-Organic Framework-808 for CO2 Capture. *Chemical Engineering Journal* **2022**, *439*, 135650.
(5) Kinik, F. P.; Altintas, C.; Balci, V.; Koyuturk, B.; Uzun, A.; Keskin, S. [BMIM][PF $_6$] Incorporation Doubles CO $_2$ Selectivity of ZIF-8: Elucidation of Interactions and Their Consequences on Performance. *ACS Appl. Mater. Interfaces* **2016**, *8* (45), 30992−31005.
(6) Fujie, K.; Otsubo, K.; Ikeda, R.; Yamada, T.; Kitagawa, H. Low Temperature Ionic Conductor: Ionic Liquid Incorporated within a Metal-Organic Framework. *Chem. Sci.* **2015**, *6* (7), 4306−4310.
(7) Nozari, V.; Calahoo, C.; Tuffnell, J. M.; Keen, D. A.; Bennett, T. D.; Wondraczek, L. Ionic Liquid Facilitated Melting of the Metal-Organic Framework ZIF-8. *Nat. Commun.* **2021**, *12* (1), 5703.
(8) Deiko, G. S.; Isaeva, V. I.; Kustov, L. M. New Molecular Sieve Materials: Composites Based on Metal-Organic Frameworks and Ionic Liquids. *Petroleum Chemistry* **2019**, *59* (8), 770−787.
(9) Sezginel, K. B.; Keskin, S.; Uzun, A. Tuning the Gas Separation Performance of CuBTC by Ionic Liquid Incorporation. *Langmuir* **2016**, *32* (4), 1139−1147.
(10) Li, H.; Tuo, L.; Yang, K.; Jeong, H.-K.; Dai, Y.; He, G.; Zhao, W. Simultaneous Enhancement of Mechanical Properties and CO2 Selectivity of ZIF-8 Mixed Matrix Membranes: Interfacial Toughening Effect of Ionic Liquid. *J. Membr. Sci.* **2016**, *511*, 130−142.
(11) Zeeshan, M.; Keskin, S.; Uzun, A. Enhancing CO2/CH4 and CO2/N2 Separation Performances of ZIF-8 by Post-Synthesis Modification with [BMIM][SCN]. *Polyhedron* **2018**, *155*, 485−492.
(12) Mohamedali, M.; Henni, A.; Ibrahim, H. Markedly Improved CO2 Uptake Using Imidazolium-Based Ionic Liquids Confined into HKUST-1 Frameworks. *Microporous Mesoporous Mater.* **2019**, *284*, 98−110.
(13) Xu, Q.; Zhang, X.; Zeng, S.; Bai, L.; Zhang, S. Ionic Liquid Incorporated Metal Organic Framework for High Ionic Conductivity over Extended Temperature Range. *ACS Sustainable Chem. Eng.* **2019**, *7* (8), 7892−7899.
(14) Fujie, K.; Yamada, T.; Ikeda, R.; Kitagawa, H. Introduction of an Ionic Liquid into the Micropores of a Metal-Organic Framework and Its Anomalous Phase Behavior. *Angew. Chem.* **2014**, *126* (42), 11484−11487.
(15) Chen, L.-H.; Wu, B.-B.; Zhao, H.-X.; Long, L.-S.; Zheng, L.-S. High Temperature Ionic Conduction Mediated by Ionic Liquid Incorporated within the Metal-Organic Framework UiO-67(Zr). *Inorg. Chem. Commun.* **2017**, *81*, 1−4.
(16) Sun, X.-L.; Deng, W.-H.; Chen, H.; Han, H.-L.; Taylor, J. M.; Wan, C.-Q.; Xu, G. A Metal-Organic Framework Impregnated with a Binary Ionic Liquid for Safe Proton Conduction above 100 °C. *Chem. -Eur. J.* **2017**, *23* (6), 1248−1252.
(17) Xu, L.; Kwon, Y.-U.; de Castro, B.; Cunha-Silva, L. Novel Mn(II)-Based Metal-Organic Frameworks Isolated in Ionic Liquids. *Cryst. Growth Des.* **2013**, *13* (3), 1260−1266.
(18) Xu, L.; Liu, B.; Liu, S.-X.; Jiao, H.; de Castro, B.; Cunha-Silva, L. The Influence of 1-Alkyl-3-Methyl Imidazolium Ionic Liquids on a Series of Cobalt-1,4-Benzenedicarboxylate Metal-Organic Frameworks. *CrystEngComm* **2014**, *16* (46), 10649−10657.
(19) Ban, Y.; Li, Z.; Li, Y.; Peng, Y.; Jin, H.; Jiao, W.; Guo, A.; Wang, P.; Yang, Q.; Zhong, C.; Yang, W. Confinement of Ionic Liquids in Nanocages: Tailoring the Molecular Sieving Properties of ZIF-8 for Membrane-Based CO $_2$ Capture. *Angew. Chem., Int. Ed.* **2015**, *54* (51), 15483−15487.
(20) Zhang, Z.-H.; Xu, L.; Jiao, H. Ionothermal Synthesis, Structures, Properties of Cobalt-1,4-Benzenedicarboxylate Metal-Organic Frameworks. *J. Solid State Chem.* **2016**, *238*, 217−222.
(21) Wang, M.-M.; Wei, Z.; Xu, L.; Liu, B.; Jiao, H. Two Temperature-Controlled Zinc Coordination Polymers: Ionothermal Synthesis, Properties, and Dye Adsorption: Two Temperature-Controlled Zinc Coordination Polymers: Ionothermal Synthesis, Properties, and Dye Adsorption. *Eur. J. Inorg. Chem.* **2018**, *2018* (7), 932−939.
(22) Khan, N. A.; Hasan, Z.; Jhung, S. H. Ionic Liquid@MIL-101 Prepared via the Ship-in-Bottle Technique: Remarkable Adsorbents for the Removal of Benzothiophene from Liquid Fuel. *Chem. Commun.* **2016**, *52* (12), 2561−2564.
(23) Ahmed, I.; Panja, T.; Khan, N. A.; Sarker, M.; Yu, J.-S.; Jhung, S. H. Nitrogen-Doped Porous Carbons from Ionic Liquids@MOF: Remarkable Adsorbents for Both Aqueous and Nonaqueous Media. *ACS Appl. Mater. Interfaces* **2017**, *9* (11), 10276−10285.
(24) Khan, N. A.; Bhadra, B. N.; Jhung, S. H. Heteropoly Acid-Loaded Ionic Liquid@metal-Organic Frameworks: Effective and Reusable Adsorbents for the Desulfurization of a Liquid Model Fuel. *Chemical Engineering Journal* **2018**, *334*, 2215−2221.
(25) Ahmed, I.; Adhikary, K. K.; Lee, Y.-R.; Ho Row, K.; Kang, K.-K.; Ahn, W.-S. Ionic Liquid Entrapped UiO-66: Efficient Adsorbent for Gd3+ Capture from Water. *Chemical Engineering Journal* **2019**, *370*, 792−799.
(26) Tu, M.; Reinsch, H.; Rodríguez-Hermida, S.; Verbeke, R.; Stassin, T.; Egger, W.; Dickmann, M.; Dieu, B.; Hofkens, J.; Vankelecom, I. F. J.; Stock, N.; Ameloot, R. Reversible Optical Writing and Data Storage in an Anthracene-Loaded Metal-Organic Framework. *Angew. Chem., Int. Ed.* **2019**, *58* (8), 2423−2427.
(27) Hermes, S.; Schröder, F.; Amirjalayer, S.; Schmid, R.; Fischer, R. A. Loading of Porous Metal-Organic Open Frameworks with Organometallic CVD Precursors: Inclusion Compounds of the Type [L $_n$ M] $_a$ @MOF-5. *J. Mater. Chem.* **2006**, *16* (25), 2464−2472.
(28) Cremer, T.; Killian, M.; Gottfried, J. M.; Paape, N.; Wasserscheid, P.; Maier, F.; Steinrück, H.-P. Physical Vapor Deposition of [EMIM][Tf $_2$ N]: A New Approach to the Modification of Surface Properties with Ultrathin Ionic Liquid Films. *ChemPhysChem* **2008**, *9* (15), 2185−2190.
(29) Hekayati, J.; Roosta, A.; Javanmardi, J. On the Prediction of the Vapor Pressure of Ionic Liquids Based on the Principle of Corresponding States. *J. Mol. Liq.* **2017**, *225*, 118−126.
(30) Kamal, A.; Chouhan, G. Investigations Towards the Chemoselective Thioacetaliztion of Carbonyl Compounds by Using Ionic Liquid[Bmim]Br as a Recyclable Catalytic Medium. *Advanced Synthesis & Catalysis* **2004**, *346* (5), 579−582.
(31) Große Böwing, A.; Jess, A. Kinetics of Single- and Two-Phase Synthesis of the Ionic Liquid 1-Butyl-3-Methylimidazolium Chloride. *Green Chem.* **2005**, *7* (4), 230−235.
(32) Obst, M.; Arnauts, G.; Cruz, A. J.; Calderon Gonzalez, M.; Marcoen, K.; Hauffman, T.; Ameloot, R. Chemical Vapor Deposition of Ionic Liquids for the Fabrication of Ionogel Films and Patterns. *Angew. Chem., Int. Ed.* **2021**, *60* (49), 25668−25673.
(33) Xiao, Y.; Hong, A. N.; Hu, D.; Wang, Y.; Bu, X.; Feng, P. Solvent-Free Synthesis of Zeolitic Imidazolate Frameworks and the Catalytic Properties of Their Carbon Materials. *Chem. -Eur. J.* **2019**, *25* (71), 16358−16365.
(34) Arellano, I. H. J.; Guarino, J. G.; Paredes, F. U.; Arco, S. D. Thermal Stability and Moisture Uptake of 1-Alkyl-3-Methylimidazolium Bromide. *J. Therm. Anal. Calorim.* **2011**, *103* (2), 725−730.

https://doi.org/10.1021/acs.inorgchem.2c02615
Inorg. Chem. 2022, 61, 17137−17143

(35) Zhang, C.; Lively, R. P.; Zhang, K.; Johnson, J. R.; Karvan, O.; Koros, W. J. Unexpected Molecular Sieving Properties of Zeolitic Imidazolate Framework-8. *J. Phys. Chem. Lett.* **2012**, *3* (16), 2130−2134.
(36) Guo, Z.; Zheng, W.; Yan, X.; Dai, Y.; Ruan, X.; Yang, X.; Li, X.; Zhang, N.; He, G. Ionic Liquid Tuning Nanocage Size of MOFs through a Two-Step Adsorption/Infiltration Strategy for Enhanced Gas Screening of Mixed-Matrix Membranes. *J. Membr. Sci.* **2020**, *605*, 118101.
(37) Stassin, T.; Verbeke, R.; Cruz, A. J.; Rodríguez-Hermida, S.; Stassen, I.; Marreiros, J.; Krishtab, M.; Dickmann, M.; Egger, W.; Vankelecom, I. F. J.; Furukawa, S.; De Vos, D.; Grosso, D.; Thommes, M.; Ameloot, R. Porosimetry for Thin Films of Metal-Organic Frameworks: A Comparison of Positron Annihilation Lifetime Spectroscopy and Adsorption-Based Methods. *Adv. Mater.* **2021**, *33* (17), 2006993.
(38) Tan, J. C.; Bennett, T. D.; Cheetham, A. K. Chemical Structure, Network Topology, and Porosity Effects on the Mechanical Properties of Zeolitic Imidazolate Frameworks. *Proc. Natl. Acad. Sci. U. S. A.* **2010**, *107* (22), 9938−9943.
(39) Kim, K.-S.; Shin, B.-K.; Lee, H. Physical and Electrochemical Properties of 1-Butyl-3-Methylimidazolium Bromide, 1-Butyl-3-Methylimidazolium Iodide, and 1-Butyl-3-Methylimidazolium Tetrafluoroborate. *Korean J. Chem. Eng.* **2004**, *21* (5), 1010−1014.
(40) Hobday, C. L.; Woodall, C. H.; Lennox, M. J.; Frost, M.; Kamenev, K.; Düren, T.; Morrison, C. A.; Moggach, S. A. Understanding the Adsorption Process in ZIF-8 Using High Pressure Crystallography and Computational Modelling. *Nat. Commun.* **2018**, *9* (1), 1429.
(41) Tietze, M. L.; Obst, M.; Arnauts, G.; Wauteraerts, N.; Rodríguez-Hermida, S.; Ameloot, R. Parts-per-Million Detection of Volatile Organic Compounds via Surface Plasmon Polaritons and Nanometer-Thick Metal-Organic Framework Films. *ACS Appl. Nano Mater.* **2022**, *5* (4), 5006−5016.
(42) Zhang, K.; Lively, R. P.; Zhang, C.; Koros, W. J.; Chance, R. R. Investigating the Intrinsic Ethanol/Water Separation Capability of ZIF-8: An Adsorption and Diffusion Study. *J. Phys. Chem. C* **2013**, *117* (14), 7214−7225.
(43) Lu, G.; Hupp, J. T. Metal-Organic Frameworks as Sensors: A ZIF-8 Based Fabry-Pérot Device as a Selective Sensor for Chemical Vapors and Gases. *J. Am. Chem. Soc.* **2010**, *132* (23), 7832−7833.

https://doi.org/10.1021/acs.inorgchem.2c02615
Inorg. Chem. 2022, 61, 17137−17143